Natural Convection Distorted Non-Newtonian Flow in a Vertical Pipe

SCOTT H. DeYOUNG and GEORGE F. SCHEELE
Cornell University, Ithaca, New York

The equations of motion and energy are solved numerically for fully developed laminar flow of a power law fluid in a vertical pipe with constant heat flux at the wall. Density is assumed to be the only temperature dependent physical property of the fluid. Temperature profiles, velocity profiles, and Nusselt numbers are presented as functions of the power law exponent and the ratio of the Grashof number divided by the Reynolds number.

The prediction of the rate of heat transfer to or from a laminar flowing non-Newtonian liquid in a smooth circular pipe is complicated by the variation of fluid physical properties with temperature. This variation will cause a distortion in the isothermal velocity profile which in turn affects the temperature field and the rate of heat transfer. Numerous studies which confirm the lack of agreement between experimental heat transfer coefficients and those predicted by constant property analyses are summarized by Metzner (*7*) and Skelland (*16*). Large profile distortions can even cause an otherwise laminar flow to become turbulent (*11*).

Several variable property analyses exist, all of which consider a temperature dependent consistency and assume that natural convection effects are negligible (*7, 16*). Many non-Newtonian liquids are so highly viscous that such an assumption is valid. However, there is experimental evidence for less viscous non-Newtonian liquids that natural convection effects may influence heat transfer rates significantly (*8, 10*). In fact, Metzner (*7*) estimates from available data that "the maximum effects due to natural convection, temperature dependence of rheological properties and non-Newtonian properties are 300%, 43% and 30%, respectively." Furthermore, the heat transfer induced flow instabilities observed at low Reynolds numbers most likely are caused by profile distortions resulting primarily from natural convection (*11*). Empirical heat transfer correlations which account for natural convection effects, such as those for flow in horizontal tubes (*8, 10*), may be satisfactory for design purposes, but they give no information about the velocity distribution and hence the stability of such flows.

In spite of the demonstrated importance of natural convection effects, no analysis exists for non-Newtonian fluids with a temperature dependent density. Any complete analysis should include both temperature varying viscosity and density, but the complexity is such that a constant viscosity analysis should be a useful preliminary step in understanding the role of natural convection. To be of value the analysis should not only predict the magnitude of the convection effect on heat transfer coefficients but should also present velocity profiles suitable for comparing hydrodynamic stability theory predictions with experimental transition results.

Constant wall flux heat transfer in vertical pipes is ideally suited to such a study when the density is the only temperature dependent fluid property because fully developed distorted velocity and temperature profiles will be attained far downstream in the heat transfer section, considerably simplifying both the analysis and subsequent experiments. For Newtonian flow, analytical solutions have been obtained for the fully developed fields (*4, 5, 9*). Of course, no fluid has a truly temperature independent viscosity, so the attainment of fully developed flow can only be approximated in any real system. For experimental conditions carefully chosen to minimize variable viscosity effects, experiments conducted with water have shown the predominance of the natural convection effect and have confirmed the essential features of the analysis (*12, 14*). These studies have contributed to the understanding of flow stability at low Reynolds numbers. It has been shown both theoretically and experimentally that the effects of viscosity variations become increasingly important as the radial viscosity gradient increases (*6*). For non-Newtonian flow with constant flux heat transfer, analytical solutions have been obtained only for fluids with temperature independent physical properties, both in the fully developed (*3*) and developing (*15*) flow regions.

This paper presents numerical solutions for velocity and temperature distributions and heat transfer coefficients for constant flux heating of a power law fluid in the fully developed region attained in a vertical pipe when density

Scott H. DeYoung is with Amoco Chemicals Corp., Whiting, Indiana.

is the only temperature varying property. The power law constitutive equation is used because of its simplicity.

THEORETICAL ANALYSIS

A quantitative description of the heat distorted velocity and temperature fields may be obtained by solving simultaneously the equations of motion and energy for an incompressible fluid, allowing the buoyancy term in the equation of motion to vary with temperature. For the fully developed flow conditions established far downstream in a vertical pipe with constant wall heat flux, the equation of motion written in terms of shear stresses reduces to

$$-\frac{dP}{dz} + \rho g_z - \frac{1}{r}\frac{d}{dr}(r\tau_{rz}) = 0 \qquad (1)$$

For small temperature changes, the density may be approximated linearly by

$$\rho = \rho_{av} + \rho_{av}\,\beta(t_{av} - t) \qquad (2a)$$

where

$$t_{av} = \left(\int_0^a trdr\right) \Big/ \; a^2 \qquad (2b)$$

This assumption limits the analysis because it has been found that for fairly severe heat transfer conditions, it is necessary to use a quadratic expression in place of Equation (2*a*) to obtain good agreement between theory and experiment (*6*). The pressure gradient can be eliminated from Equation (1) by using the overall force balance

$$\tau_w = -\frac{a}{2}\frac{dP}{dz} + \frac{\rho_{av}\,g_z a}{2} \qquad (3)$$

If Equations (2*a*) and (3) are substituted into Equation (1), if the dimensionless variables $R = r/a$ and $\tau' = \tau_{rz}/\tau_w$ are introduced, and if g_z is replaced by g, the equation of motion becomes

$$d(R\tau') = \left[2 \pm \frac{a\rho_{av}\,g\beta(t - t_{av})}{\tau_w}\right] RdR \qquad (4)$$

where the positive sign represents upflow and the negative sign downflow.

Equation (4) is general until a constitutive equation is specified. For a power law fluid (*1*)

$$\tau_{rz} = -K\left|\frac{dv}{dr}\right|^{\alpha-1}\frac{dv}{dr} = \pm K\left|\frac{dv}{dr}\right|^{\alpha} \qquad (5)$$

The positive sign is associated with a negative velocity gradient and vice versa. Both the consistency K and the index α, which are functions of temperature, are assumed constant in the subsequent analysis. Neglecting the temperature variation of α is a good assumption, but considering K a constant significantly limits the analysis because K can be a strong function of temperature (*17*).

The wall shear stress is obtained by evaluating Equation (5) at $r = a$; it may then be substituted into Equation (4). If, in addition, a dimensionless velocity $V = v/v_{av}$, a dimensionless temperature $T = k(t - t_{av})/qa$, and an effective viscosity $\mu_{eff} = K(v_{av}/a)^{\alpha-1}$ are defined, the equation of motion can be expressed in terms of dimensionless variables and parameters as

$$d(R\tau') = 2 + \left[\frac{N_{Gr}\,T}{N_{Re}\left|\frac{dV}{dR}\right|^{\alpha}_{R=1}}\right] RdR \qquad (6)$$

where

$$N_{Gr} = a^4\,\rho_{av}^2\,g\beta q/k\,\mu^2_{eff} \qquad (7a)$$

$$N_{Re} = a\,v_{av}\rho_{av}/\mu_{eff} \qquad (7b)$$

Because of the two sign possibilities in both Equations (4) and (5), use of the positive sign in Equation (6) is valid only when the following convention on the ratio N_{Gr}/N_{Re} is adopted. For liquids with a positive coefficient of thermal expansion β, the ratio is positive for upflow heating and for downflow heating with a positive wall velocity gradient; for downflow heating with a negative wall velocity gradient, the ratio is negative. For constant flux cooling the convention is reversed.

In terms of the previously defined dimensionless variables, the energy equation reduces to

$$\frac{d^2T}{dR^2} + \frac{1}{R}\frac{dT}{dR} = 2V \qquad (8)$$

and the equation of continuity for an incompressible liquid becomes

$$\int_0^1 VR\;dR = ½ \qquad (9)$$

The following boundary conditions must also be satisfied:

$$dT/dR = 0 \quad \text{at} \quad R = 0 \qquad (10a)$$

$$dV/dR = 0 \quad \text{at} \quad R = 0 \qquad (10b)$$

$$V = 0 \quad \text{at} \quad R = 1 \qquad (10c)$$

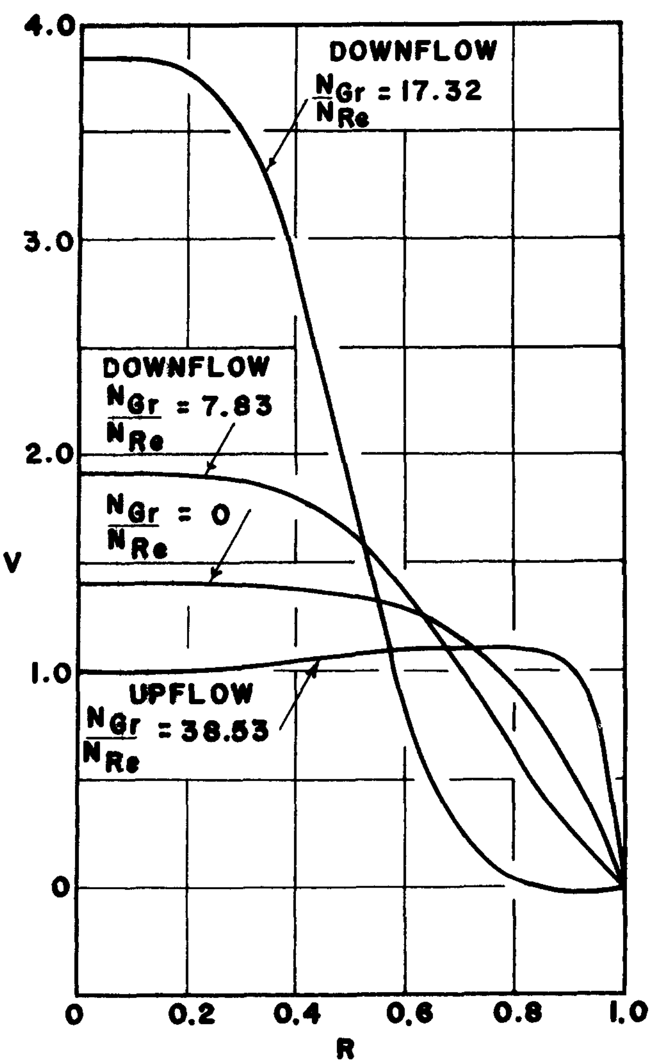

Fig. 1. Natural convection distorted velocity profiles for $\alpha = 0.25$ as a function of N_{Gr}/N_{Re}.

Equations (5), (6), (8), and (9) together with the boundary conditions define the problem. Once the velocity and temperature profiles have been determined, the Nusselt number based on the difference between the wall and mixing cup average temperatures can be calculated from

$$N_{Nu} = hd/k = 2 \bigg/ \left(T_w - 2 \int_0^1 TVRdR \right) \quad (11)$$

For fluids with a temperature independent density, the second term on the right side of Equation (6) is zero because $N_{Gr} = 0$, and if the viscosity is also temperature independent, the motion and energy equations are no longer coupled. Analytical solutions for the velocity and temperature fields exist for both Newtonian (*1*) and power law fluids (*3*), as well as for non-Newtonian fluids whose rheological behavior is described by other constitutive equations (*15*).

For variable density fluids, analytical solutions have been obtained only for the Newtonian case ($\alpha = 1$) by several investigators (*4, 5, 9*). The treatment of Hanratty, Rosen, and Kabel (*5*) is recommended for those interested in details of the solution. The profiles are functions of N_{Gr}/N_{Re}. For non-Newtonian fluids, a numerical solution of the coupled equations is necessary to predict the profiles as functions of N_{Gr}/N_{Re} and the index α.

NUMERICAL SOLUTION

The finite difference technique for obtaining a solution was facilitated by rewriting Equation (6) as

$$d(R\tau') = (2 + GT)RdR \quad (12)$$

The solution was performed for given values of α and G. The choice of G rather than N_{Gr}/N_{Re} as the input parame-

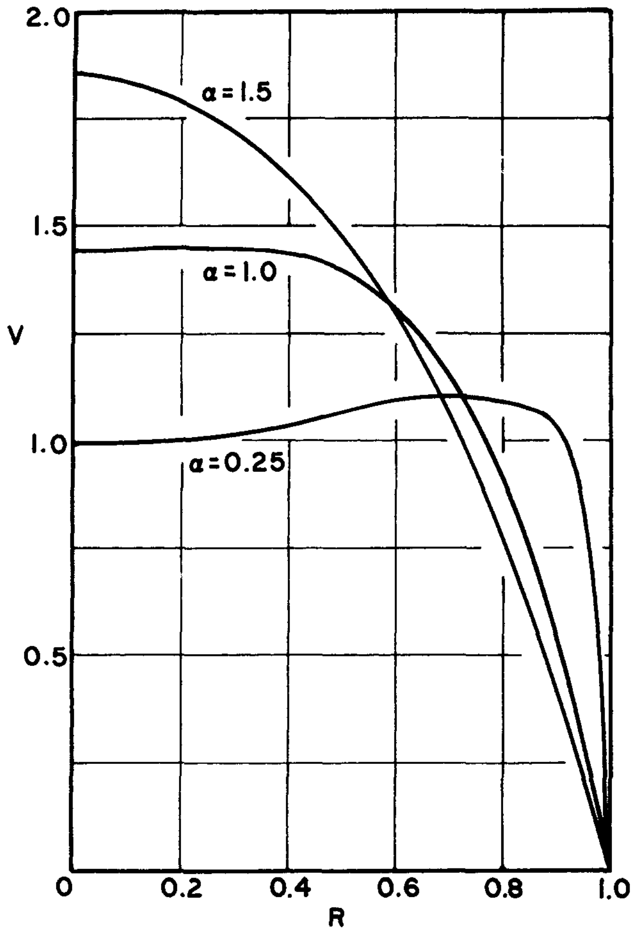

Fig. 3. Upflow heating distorted velocity profiles for N_{Gr}/N_{Re} = 38.5 as a function of α.

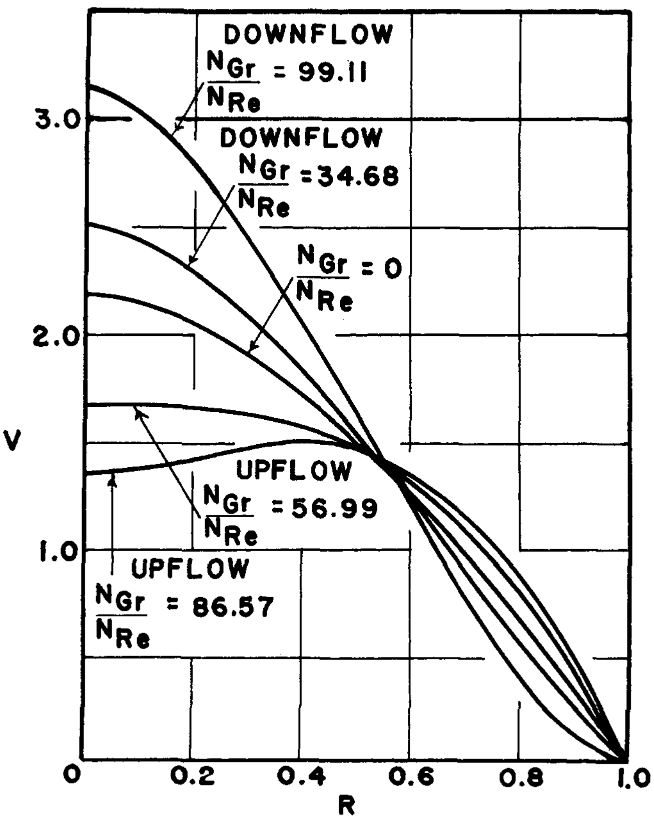

Fig. 2. Natural convection distorted velocity profiles for α = 1.50 as a function of N_{Gr}/N_{Re}.

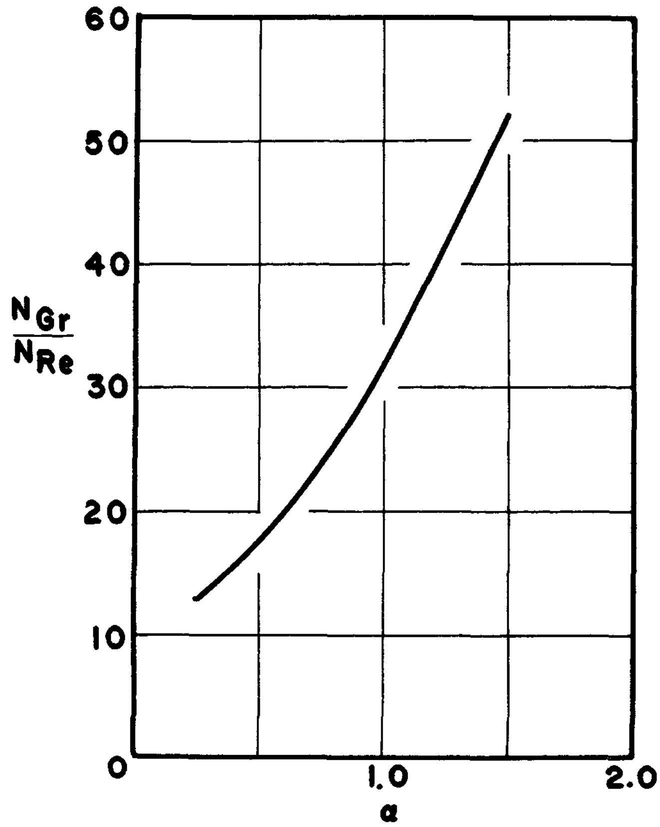

Fig. 4. N_{Gr}/N_{Re} ratio at which maximum velocity first moves off center as a function of α for upflow heating.

ter improved convergence. An assumed initial velocity profile was used to obtain a temperature profile from the energy equation, Equation (8), by using a fourth-order Runge-Kutta integration method. The temperature profile was then substituted into the equation of motion, Equation (12), to obtain a shear stress distribution, which in turn was used with the constitutive equation, Equation (5), to obtain a better estimate of the velocity distribution. The calculations were repeated until the center-line velocities from two successive calculations agreed within 0.002%. After the velocity and temperature profiles were determined, N_{Gr}/N_{Re} was calculated from the G value and the wall velocity gradient. Finally, the Nusselt number was computed by numerical integration of Equation (11).

A Fortran IV computer program was developed, and an IBM 360-65 digital computer was used to solve the equations. Details of the procedure and the computer program are presented elsewhere (2). The program satisfactorily computed all profiles of interest. However, for large positive N_{Gr}/N_{Re} ratios, the solutions converged to profiles associated with negative ratio flows. Since this occurred only for conditions where the maximum local velocity would be far off center, such solutions were of only marginal value because of the demonstrated experimental instability of such Newtonian flow fields (*12*), and no attempt was made to improve the convergence.

The procedure described requires an initial estimate of the velocity distribution. It was found that the initial estimate had no effect on the final results but that computer time was minimized when the analytical Newtonian profile associated with the given G value was used.

The analytical solutions for variable density Newtonian fluids and for constant property power law fluids were used to verify the numerical calculations. The agreement of better than 0.1% in all cases indicated that a stepsize $\Delta R = 0.01$ and single precision computing were adequate for the calculations.

NUMERICAL RESULTS

Numerical solutions were obtained for α values from 0.25 to 1.50 in increments of 0.25, values that should include most liquids of practical interest. Upflow N_{Gr}/N_{Re} ratios were varied from zero to values where the maximum local velocity had moved significantly off center, while downflow ratios were varied from zero to values where flow reversal occurred at the wall.

The fully developed velocity profiles for several representative N_{Gr}/N_{Re} ratios are shown in Figures 1 and 2 for a pseudoplastic liquid with $\alpha = 0.25$ and a dilatant liquid with $\alpha = 1.50$, respectively. The profiles for $N_{Gr}/N_{Re} = 0$ are the isothermal or constant property velocity distributions. The features of the heat distorted profiles are similar for all α values. For upflow heating the wall velocity gradient increases from the isothermal value as the ratio of heat input to flow rate increases, while the center-line velocity correspondingly decreases. At moderate values of N_{Gr}/N_{Re}, the maximum velocity moves off center. For downflow heating, the wall velocity gradient decreases with increasing N_{Gr}/N_{Re}, and the center-line velocity increases. For moderate values of the ratio, a reversal of flow near the wall is predicted.

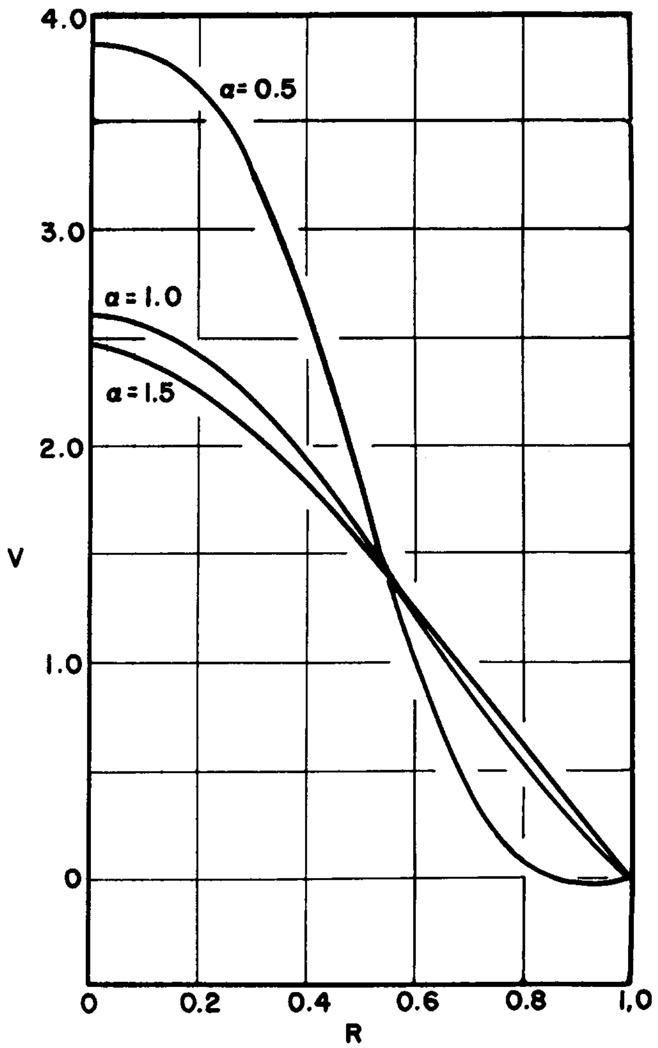

Fig. 5. Downflow heating distorted velocity profiles for $N_{Gr}/N_{Re} = 29.8$ as a function of α.

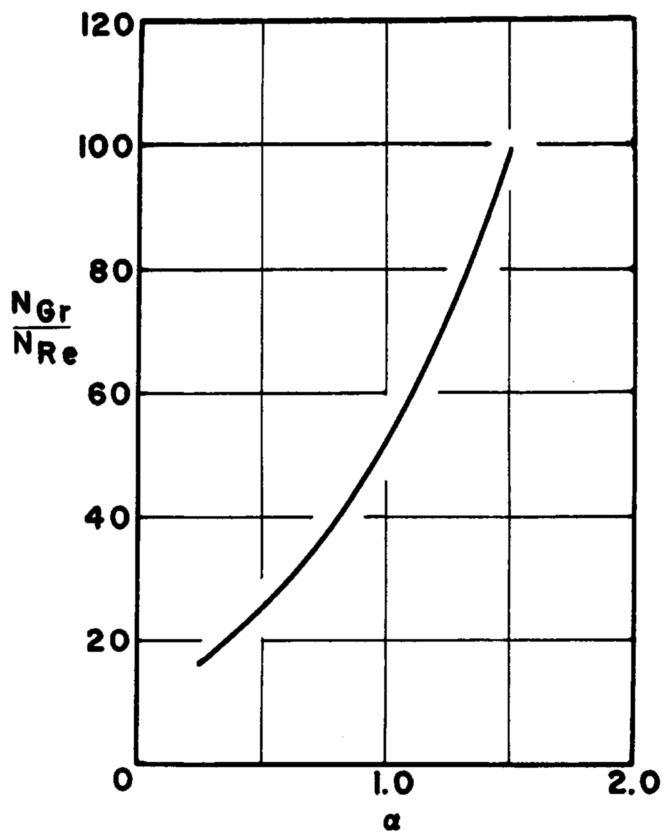

Fig. 6. N_{Gr}/N_{Re} ratio at which wall velocity gradient becomes zero as a function of α for downflow heating.

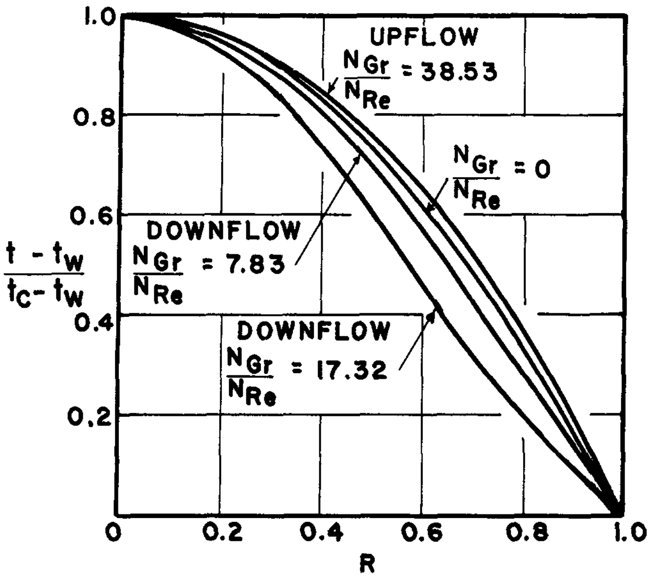

Fig. 7. Heat distorted temperature profiles for α = 0.25 as a function of N_{Gr}/N_{Re}.

In spite of the similarity of effects associated with all α values, the degree of non-Newtonian behavior characterized by the index α has a significant effect on the velocity field at a given N_{Gr}/N_{Re} ratio. For isothermal profiles, decreasing α increases the bluntness of the velocity profiles. Figure 3 shows the effect of α on the flow field for upflow heating with $N_{Gr}/N_{Re} = 38.5$. For the heat distorted profiles, a decrease in α enhances the blunting effect associated with the natural convection phenomenon.

Associated with the increasing bluntness of the velocity distribution is a decrease in the critical N_{Gr}/N_{Re} ratio at which the maximum velocity first moves off center. In Figure 3 the maximum velocity has already moved off center for the two lowest α values, while the maximum velocity is still at the center of the pipe for $\alpha = 1.50$. Figure 4 shows the increase in the critical ratio with increasing α from 12.8 at $\alpha = 0.25$ to 52 at $\alpha = 1.50$. For Newtonian fluids, it has been found experimentally that the flow is unstable and becomes turbulent for ratios greater than the critical value (*6*, *12*). If the critical ratio also

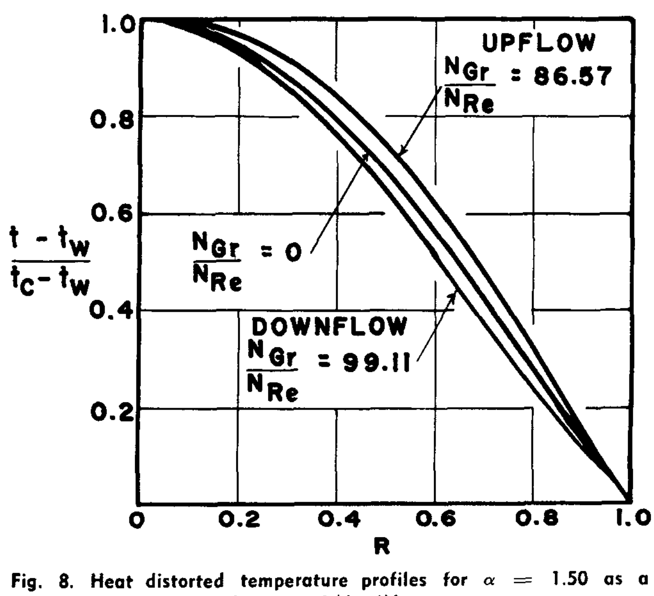

Fig. 8. Heat distorted temperature profiles for α = 1.50 as a function of N_{Gr}/N_{Re}.

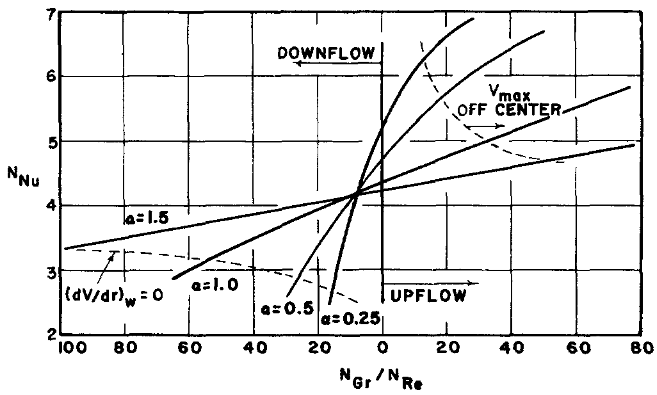

Fig. 9. Nusselt numbers for upflow and downflow heating.

defines the stability limits for non-Newtonian liquids, then, in long pipes, flows below the curve in Figure 4 will remain laminar at low Reynolds numbers, while those above will become turbulent. From this stability criterion, the limiting stable N_{Gr}/N_{Re} will be lower for pseudoplastic than for dilatant fluids.

Figure 5 shows the effect of α on the velocity distribution for downflow heating with $N_{Gr}/N_{Re} = 29.8$. The interaction of the non-Newtonian and natural convection effects is such that while at low ratios, the maximum centerline velocity increases with increasing α, at high ratios the lowest α fluid is predicted to have the largest center line velocity.

For $\alpha = 0.5$ and a ratio of 29.8, a reverse flow at the wall is predicted, while for the larger α values shown no reversal is predicted. Figure 6 shows the value of the critical N_{Gr}/N_{Re} ratio at which the wall velocity gradient becomes zero as a function of α. The critical ratio increases with increasing α from 15.9 at $\alpha = 0.25$ to 99.1 at $\alpha = 1.50$. For ratio values larger than the critical, flow separation and instability have been observed experimentally for Newtonian liquids (*12*) and would be expected to occur also for non-Newtonian liquids. It appears that for downflow as well as upflow, the limiting stable N_{Gr}/N_{Re} value is lower for pseudoplastic than for dilatant fluids.

Figures 7 and 8 show the temperature profiles for $\alpha = 0.25$ and 1.50, respectively, which are associated with velocity profiles shown in Figures 1 and 2. Because of the method chosen for nondimensionalizing the temperature profiles which forces all profiles to be 1.0 at the center of the pipe and 0.0 at the wall, the effect of a change in N_{Gr}/N_{Re} or α on the temperature distribution appears to be much less than the corresponding effect on the velocity distribution.

In spite of the apparent insensitivity of the temperature profiles, changes in N_{Gr}/N_{Re} and α do have a significant effect on the heat transfer coefficient. Figure 9 shows the large effects of N_{Gr}/N_{Re} and α on the Nusselt number for both upflow and downflow heating. The region between the dotted lines showing the critical N_{Gr}/N_{Re} ratios for both upflow and downflow heating defines the expected stable flow region in long pipes, within which the laminar analysis is likely to be applicable. For larger N_{Gr}/N_{Re} ratios, turbulent flow would likely lead to higher heat transfer coefficients.

For all α values, N_{Nu} increases with N_{Gr}/N_{Re} for upflow heating because of the increasing wall velocity gradient, as seen in Figures 1 and 2, while for downflow heating the opposite is true. The justification often used for neglecting convection effects in theoretical analyses, namely that the predictions will lead to conservative estimates of the heat transfer rate, is clearly invalid for downflow heating. The change in N_{Nu} over the predicted laminar region is greatest for $\alpha = 0.25$ and decreases with increasing α, because the maximum distortion of the isothermal velocity profile within the laminar region is less for dilatant than for pseudoplastic liquids.

For upflow heating, N_{Nu} decreases with increasing α for all N_{Gr}/N_{Re} values because of the corresponding decrease in the wall velocity gradient, as shown in Figure 3 for $N_{Gr}/N_{Re} = 38.5$. The situation is more complex for downflow heating. At low N_{Gr}/N_{Re} values, smaller α's give larger wall velocity gradients, while the reverse is true at high ratios. Consequently, there is an intersection of the curves on Figure 9 in the region of $N_{Gr}/N_{Re} = 8$ to 10.

SUMMARY

Theoretical velocity and temperature profiles and Nusselt numbers have been presented as functions of the power law index and the ratio of Grashof to Reynolds number for fully developed laminar flow of a non-Newtonian liquid with temperature varying density in a vertical pipe undergoing constant flux heating at the wall. No experimental results for such systems exist in the literature, so direct comparison of the numerical results with data is not possible. However, some qualitative similarities with data suggest the validity of the analysis.

The Nusselt numbers increase for upflow heating and decrease for downflow heating with respect to the constant fluid property values. The natural convection effect is largest for pseudoplastic and smallest for dilatant liquids, and its magnitude is consistent with the large natural convection effects found experimentally (*7, 8, 10*).

For upflow heating, the velocity profile distortion is such that the maximum velocity finally moves off center for high heat fluxes for all values of the power law index, while for downflow heating reverse flow ultimately occurs at the pipe wall. Since both conditions have been found to produce instability for Newtonian liquids, the prediction of such profiles for non-Newtonian liquids is consistent with the experimentally observed transition to turbulent flow for power law liquids at low Reynolds numbers (*11*). The range of predicted stable N_{Gr}/N_{Re} ratios is smallest for pseudoplastic and largest for dilatant liquids.

Natural convection induced turbulence will have a practical effect on heat transfer rates which depends on the relative magnitudes of the laminar and turbulent flow wall velocity gradients. For Newtonian liquids, the induced turbulence significantly increases heat transfer rates for downflow heating but has only a slight effect for upflow heating, where the laminar wall velocity gradients are already large (*13*). The same general results are likely for non-Newtonian liquids, although for upflow heating of highly pseudoplastic liquids, a reduction in the Nusselt number may accompany transition to turbulence.

Because of the encouraging nature of the preliminary comparisons, experiments taken under conditions approximating the analysis will be the subject of a future paper.

ACKNOWLEDGMENT

The authors thank Dr. J. S. Vrentas of The Dow Chemical Company for his suggestions concerning the numerical analysis.

NOTATION

a = pipe radius, cm.
d = pipe diameter, cm.
g = acceleration of gravity, 980 cm./sec.^{2}
g_z = component of gravitational acceleration in flow direction, cm./sec.^{2}
G = dimensionless parameter in Equation (12) = $N_{Gr}/(N_{Re}|dV/dR|^{\alpha}{}_{R=1})$
h = heat transfer coefficient based on difference between wall and mixing cup average temperatures, cal./(sec.)(sq.cm.)(°C.)
k = fluid thermal conductivity, cal./(sec.)(cm.)(°C.)
K = non-Newtonian liquid consistency, g./(cm.)(sec.)$^{2-\alpha}$
N_{Gr} = Grashof number defined by Equation (*7a*)
N_{Nu} = Nusselt number defined by Equation (11)
N_{Re} = Reynolds number defined by Equation (*7b*)
P = fluid pressure, g./(cm.)(sec.)^2
q = wall heat flux, cal./(sq.cm.)(sec.)
r = radial distance, cm.
R = dimensionless radial distance, r/a
t = fluid temperature, °C.
t_{av} = radial average fluid temperature defined by Equation (*2b*)
t_c = center-line temperature, °C.
t_w = wall temperature, °C.
T = dimensionless fluid temperature = $k(t - t_{av})/qa$
T_w = dimensionless wall temperature
v = local axial velocity, cm./sec.
v_{av} = average fluid velocity, cm./sec.
V = dimensionless fluid velocity = v/v_{av}
z = axial distance, cm.

Greek Letters

α = dimensionless power law index
β = coefficient of volumetric expansion, °C.$^{-1}$
μ_{eff} = effective non-Newtonian viscosity = $K(v_{av}/a)^{\alpha-1}$, g./(cm.)(sec.)
ρ = local fluid density, g./cc.
ρ_{av} = radial average density, g./cc.
τ_{rz} = radial shear stress in axial direction, g./(cm.)(sec.)^2
τ_w = wall shear stress, g./(cm.)(sec.)^2
τ' = dimensionless radial shear stress = τ/τ_w

LITERATURE CITED

1. Bird, R. B., W. E. Stewart, and E. N. Lightfoot, "Transport Phenomena," Wiley, New York (1960).
2. DeYoung, S. H., M.S. thesis, Cornell Univ., Ithaca, N. Y. (1968).
3. Grigull, U., *Chem. Ingr.-Tech.*, **28**, 553, 655 (1956).
4. Hallman, T. M., *Trans. Am. Soc. Mech. Engrs.*, **78**, 1831 (1956).
5. Hanratty, T. J., E. M. Rosen, and R. L. Kabel, *Ind. Eng. Chem.*, **50**, 815 (1958).
6. Lawrence, W. T., and J. C. Chato, *J. Heat Trans.*, **88**, 214 (1966).
7. Metzner, A. B., in "Advances in Heat Transfer," Vol. 2, Academic Press, New York (1965).
8. ———, and D. F. Gluck, *Chem. Eng. Sci.*, **12**, 185 (1960).
9. Morton, B. R., *J. Fluid Mech.*, **8**, 227 (1960).
10. Oliver, D. R., and V. G. Jenson, *Chem. Eng. Sci.*, **19**, 115 (1964).
11. Scheele, G. F., and H. L. Greene, *AIChE J.*, **12**, 737 (1966).
12. Scheele, G. F., and T. J. Hanratty, *J. Fluid Mech.*, **14**, 244 (1962).
13. ————, *AIChE J.*, **9**, 183 (1963).
14. Scheele, G. F., E. M. Rosen, and T. J. Hanratty, *Can. J. Chem. Eng.*, **38**, 67 (1960).
15. Schenk, J., and J. Van Laar, *Appl. Sci. Res.*, **A7**, 449 (1958).
16. Skelland, A. H. P., "Non-Newtonian Flow and Heat Transfer," Chapt. 10, Wiley, New York (1965).
17. Turian, R. M., *Chem. Eng. Sci.*, **20**, 771 (1965).

Manuscript received October 22, 1968; revision received February 7, 1969; paper accepted February 14, 1969.